

See discussions, stats, and author profiles for this publication at: <https://www.researchgate.net/publication/5986813>

Surface Hydrophobicity Modulates the Operation of Actomyosin-Based Dynamic Nanodevices

ARTICLE *in* LANGMUIR · NOVEMBER 2007

Impact Factor: 4.46 · DOI: 10.1021/la700412m · Source: PubMed

CITATIONS

22

READS

39

8 AUTHORS, INCLUDING:



Dan Nicolau

McGill University

102 PUBLICATIONS 719 CITATIONS

SEE PROFILE



Florin Fulga

Tritagama Consult

30 PUBLICATIONS 107 CITATIONS

SEE PROFILE



Elena P. Ivanova

Swinburne University of Technology

308 PUBLICATIONS 4,392 CITATIONS

SEE PROFILE



Cristobal dos Remedios

University of Sydney

93 PUBLICATIONS 1,164 CITATIONS

SEE PROFILE

Surface Hydrophobicity Modulates the Operation of Actomyosin-Based Dynamic Nanodevices

Dan V. Nicolau,^{*,†} Gerardin Solana,[‡] Murat Kekic,[§] Florin Fulga,[†] Chitladda Mahanivong,[‡] Jonathan Wright,[‡] and Cristobal G. dos Remedios[§]

Department of Electrical Engineering and Electronics, The University of Liverpool, Liverpool, L69 3GJ, U.K., Industrial Research Institute Swinburne, Swinburne University of Technology, Hawthorn, Vic, 3122, Australia, and Muscle Research Unit, Institute for Biomedical Research, The University of Sydney, Sydney NSW 2006, Australia

Received February 12, 2007. In Final Form: July 27, 2007

We studied the impact of surface hydrophobicity on the motility of actin filaments moving on heavy-meromyosin (HMM)-coated surfaces. Apart from nitrocellulose (NC), which is the current standard for motility assays, all materials tested are good candidates for microfabrication: hydrophilic and hydrophobic glass, poly(methyl methacrylate) (PMMA), poly(*tert*-butyl methacrylate) (PtBuMA), and a copolymer of *O*-acryloyl acetophenone oxime with a 4-acryloyloxybenzophenone (AAPO). The most hydrophilic (hydrophilic glass, contact angle 35°) and the most hydrophobic (PtBuMA, contact angle 78°) surfaces do not maintain the motility of actin filaments, presumably because of the low density of adsorbed HMM protein or its high levels of denaturation, respectively. The velocity of actin filaments presents higher values in the middle of this “surface hydrophobicity motility window” (NC, PMMA), and a bimodal distribution, which is more apparent at the edges of this motility window (hydrophobic glass and AAPO). A molecular surface analysis of HMM and its S1 units suggests that the two very different, temporally separated conformations of the HMM heads could exacerbate the surface-modulated protein behavior, which is common to all microdevices using surface-immobilized proteins. An explanation for the above behavior proposes that the motility of actin filaments on HMM-functionalized surfaces is the result of the action of three populations of motors, each in a different surface–protein conformation, that is, HMM with both heads working (high velocities), working with one head (low velocities), and fully denatured HMM (no motility). It is also proposed that the molecularly dynamic nature of polymer surfaces amplifies the impact of surface hydrophobicity on protein behavior. The study demonstrates that PMMA is a good candidate for the fabrication of future actomyosin-driven dynamic nanodevices because it induces the smoothest motility of individual nano-objects with velocities comparable with those obtained on NC.

1. Introduction

Motile systems based on protein linear molecular motors (i.e., actin–myosin, microtubule–kinesin or –dynein) are ubiquitous nanomachines responsible for biological functions as diverse as cell movement and division, the transport of vesicles, and muscle function.¹ These remarkable nanomechanical machines use adenosinetriphosphate (ATP) to transform chemical energy directly into mechanical energy with high yield and spatial precision. These nanomechanical characteristics motivate increasing attempts to emulate or integrate protein molecular motors in hybrid dynamic nanodevices, which are capable of moving cargos with nanometer precision or offering a seamless technological route to single-molecule devices.²

Both fundamental studies of linear molecular motors with medical, biological, and biophysical motivations (recently comprehensively reviewed^{1,2}) and applied studies with nanotechnology and nanoengineering motivations (also reviewed recently^{3,4}) have been well served by the development of *in vitro* motility assays. The simpler, more common “gliding” architecture (proposed for actin–myosin systems^{5–7}) consists of surface-

adsorbed motor proteins (e.g., myosin or heavy meromyosin (HMM)) that propel the actin filaments, which move on a plane above the immobilized motors. Both kinesin–microtubule and myosin–actin filament systems have been used for prototype devices, but the use of the former is more common because of the easier production of kinesin and the higher rigidity and larger dimensions of microtubules (which alleviates the problems of fabrication, observation, and motility confinement). The myosin–actin system, however, has specific advantages, in particular the higher velocity of and the higher force exerted upon the motile elements, which would permit a more rapid transduction and higher transport capacity of future dynamic nanodevices.

Many devices based on linear motors use the confinement of the filament (or microtubule) motility, for example, using simple microstructures^{8–13} or nanostructures,¹⁴ molecular selectors,^{15–17}

* Corresponding author.

[†] The University of Liverpool.

[‡] Swinburne University of Technology.

[§] The University of Sydney.

(1) Howard, J. *Mechanics of Motor Proteins and the Cytoskeleton*; Sinauer Associates, Inc.: Sunderland, MA, 2001.

(2) Schliwa, M. *Molecular Motors*; Wiley-VCH: Weinheim, Germany, 2003.

(3) Kinbara, K.; Aida, T. *Chem. Rev.* **2005**, *105*, 1377–1400.

(4) Bakewell, D. J. G.; Nicolau, D. V. *Aust. J. Chem.* **2007**, *60*, 314–332.

(5) Yanagida, T.; Nakase, M.; Nishiyama, K.; Oosawa, F. *Nature* **1984**, *307*, 58–60.

(6) Kron, S. J.; Spudich, J. A. *Proc. Natl. Acad. Sci. U.S.A.* **1986**, *83*, 6272–6276.

(7) Kron, S. J.; Toyoshima, Y. Y.; Uyeda, T. Q. P.; Spudich, J. A. *Methods Enzymol.* **1991**, *196*, 399–416.

(8) Suzuki, H.; Oiwa, K.; Yamada, A.; Sakakibara, H.; Nakayama, H.; Mashiko, S. *Jpn. J. Appl. Phys., Part 1* **1995**, *34*, 3937–3941.

(9) Suzuki, H.; Yamada, A.; Oiwa, K.; Nakayama, H.; Mashiko, S. *Biophys. J.* **1997**, *72*, 1997–2001.

(10) Riveline, D.; Ott, A.; Julicher, F.; Winkelmann, D. A.; Cardoso, O.; Lacapere, J. J.; Magnusdottir, S.; Viovy, J. L.; Gorre-Talini, L.; Prost, J. *Eur. Biophys. J. Biophys. Lett.* **1998**, *27*, 403–408.

(11) Riveline, D.; Wiggins, C. H.; Goldstein, R. E.; Ott, A. *Phys. Rev. E* **1997**, *56*, R1330–R1333.

(12) Mahanivong, C.; Wright, J. P.; Kekic, M.; Pham, D. K.; dos Remedios, C. G.; Nicolau, D. V. *Biomed. Microdevices* **2002**, *4*, 111–116.

(13) Nicolau, D. V.; Suzuki, H.; Mashiko, S.; Taguchi, T.; Yoshikawa, S. *Biophys. J.* **1999**, *77*, 1126–1134.

(14) Bunk, R.; Sundberg, M.; Mansson, A.; Nicholls, I. A.; Omling, P.; Tagerud, S.; Montelius, L. *Nanotechnology* **2005**, *16*, 710–717.

and motility directed by external forces.^{10,18–24} Despite this progress, the characteristics of actin filaments (i.e., small diameters and high flexibility) makes the control of their mobility more challenging, requiring nontrivial fabrication.^{25,26} There are however other nanodevices where the above difficulties are not critical or not at all relevant. For instance, some recently proposed biosensing devices^{27,28} monitor the spatially unrestricted but molecularly modulated movement of microtubules or filaments on homogeneous planar surfaces.

Regardless of the design of molecular motor-powered devices, the choice of material has to consider both fabrication and operational issues. Nitrocellulose (NC), which has been the current standard for motility assays,^{5,6} is not appropriate for microfabricated devices, and therefore several other materials have been tested. Polymers (mostly acrylates,^{9,10,13,16} but also nanostructured Teflon,^{8,29} photoresists and e-beam resists,^{12,25} and semiconductor or related materials^{30–32}) demonstrated biocompatibility with actin–myosin motors, but the relationship between surface properties and motility characteristics was only briefly studied.^{13,30} If the nanodevices based on molecular motors are to follow the same evolution as the lab-on-a-chip devices, then polymers appear to be very attractive materials because of their manufacturability (including for nanofabrication) and low cost.

One aspect regarding molecular motor-based devices that has not received adequate attention is that they are largely parallel, single-molecule devices, where *individual* motile elements move on surfaces and perform functions as the result of the cooperative action of motor proteins randomly *distributed* on the device surface. Few reports^{13,30,32} systematically studied the surface-modulated motility behavior, but did so in the context of global motility attributes (e.g., average velocity). It follows that the behavior of individual motile elements, mediated by motor protein bioactivity and, in turn, modulated by surfaces, has to be thoroughly assessed and understood to allow for a systematic progress of hybrid nanodevices based on molecular linear motors beyond tentative prototypes.

This communication reports on the study of the effect of several surfaces (which are good candidate materials for micro/nanofabrication) on the motility of actin filaments moving on

HMM immobilized on surfaces. It has been found that the motility is suppressed by low and high surface hydrophobicity. Further, molecular level considerations and statistical analysis of the motility have been used to advance the understanding of the modulation of motility by molecular motors immobilized on surfaces. More detailed statistical analysis corroborated with the molecular surface analysis revealed and explained the presence of a bimodal distribution of the actin filaments velocity, which was further articulated in a proposed model for the motility on HMM-functionalized surfaces. This contribution concludes with a discussion on the perspectives of dynamic nanodevices based on protein molecular motors.

2. Methods and Materials

Surface Preparation and Characterization. Six surfaces (chemical structures presented in the Supporting Information) were used to test the modulation of motility: hydrophilic glass, hydrophobic glass, NC, poly(methyl methacrylate) (PMMA), poly(*tert*-butyl methacrylate) (PtBuMA), and a copolymer comprising *O*-acryloyl acetophenone oxime copolymerized with a 4-acryloyloxybenzophenone (AAPO). All materials have been used previously for actin–myosin motility and are good candidates for the microfabrication of biodevices (NC being the notable exception). In line with the specific interest of this contribution (robust and cost-effective devices based on molecular motors), most of the materials tested are polymers.

The hydrophilic glass surface was obtained by the thorough cleaning of glass slides by sonication (30 min) in isopropanol (Sigma Aldrich) washed with large amounts of Nanopure water (18.2 MΩ cm^{−1}). The hydrophobic glass was obtained by spin coating hexamethyldisilazane (Sigma-Aldrich) on a glass surface and subsequently baking it at 100 °C for 30 min. NC solution (10% in amyl acetate) was purchased (from Ernest F. Fullam) then diluted to 5% (same solvent). AAPO, synthesized according to the procedure described elsewhere³³ (molecular weight as measured by gel permeation chromatography (GPC), 1.9×10^5), was provided by Drs. K. Suyama, M. Shirai, and M. Tsunooka from Osaka Prefecture University. PMMA and PtBuMA, purchased from Sigma-Aldrich (Fluka), have molecular weights (GPC standard) of 1.6×10^5 and 1.9×10^5 , respectively. Polymer solutions (5%) of AAPO, PMMA, and PtBuMA were prepared by dissolving the polymer in cyclohexanone (Sigma Aldrich). All polymer solutions (five different batches for each polymer) were used to coat hydrophobic glass slides via spin coating at 3000 rpm for 40 s (Specialty Coating Systems P6708 spin coater). The substrates (20 slides, in the case of polymers, 4 slides/batch) for each model surface, were soft baked in a vacuum oven for 30 min at 85 °C, then placed in a desiccator for storage. In order to remove all possibilities of toxic contaminants diffusing in the motility flow cell, all substrates were stored for long periods of time (more than 1 month) prior to contact angle measurements and motility experiments. This precaution proved particularly useful for AAPO substrates.

Contact angles were measured on sessile drops (2 μL) of Nanopure water at room temperature (23–25 °C) in air using a Ramé-Hart contact angle goniometer (model 100-00-115). The contact angle values (Table 1) were averaged over ten different readings (all within ±5%) on each surface.

The nanotopography of the surfaces was measured with an atomic force microscope (AFM, Explorer model, ThermoMicroscopes) in tapping mode. The built-in software of the AFM was used to calculate the average height and root-mean-square (rms) values (Table 1).

Motility Assays. The experimental procedures for the preparation of protein and motility assays used in this study is an adaptation of

(15) Hiratsuka, Y.; Tada, T.; Oiwa, K.; Kanayama, T.; Uyeda, T. Q. P. *Biophys. J.* **2001**, *81*, 1555–1561.

(16) Oiwa, K. In *THERMEC 2003*; Trans Tech Publications: Zurich, Switzerland, 2003; Parts 1–5, Vol. 426–432, pp 2339–2344.

(17) van den Heuvel, M. G. L.; Butcher, C. T.; Smeets, R. M. M.; Diez, S.; Dekker, C. *Nano Lett.* **2005**, *5*, 1117–1122.

(18) Stracke, R.; Bohm, K. J.; Wollweber, L.; Tuszyński, J. A.; Unger, E. *Biochem. Biophys. Res. Commun.* **2002**, *293*, 602–609.

(19) Asokan, S. B.; Jawerth, L.; Carroll, R. L.; Cheney, R. E.; Washburn, S.; Superfine, R. *Nano Lett.* **2003**, *3*, 431–437.

(20) Moorjani, S. G.; Jia, L.; Jackson, T. N.; Hancock, W. O. *Nano Lett.* **2003**, *3*, 633–637.

(21) Hutchins, B. M.; Platt, M.; Hancock, W. O.; Williams, M. E. *Small* **2007**, *3*, 126–131.

(22) van den Heuvel, M. G. L.; Butcher, C. T.; Lemay, S. G.; Diez, S.; Dekker, C. *Nano Lett.* **2005**, *5*, 235–241.

(23) van den Heuvel, M. G. L.; De Graaff, M. P.; Dekker, C. *Science* **2006**, *312*, 910–914.

(24) Hanson, K. L.; Solana, G.; Nicolau, D. V. *Imaging, Manipulation, and Analysis of Biomolecules and Cells: Fundamentals and Applications III*; Nicolau, D. V., Enderlein, J., Leif, R. C., Farkas, D. F., Raghavachari, R., Eds.; SPIE Publications: Bellingham, WA, 2005; pp 196–201.

(25) Bunk, R.; Klinth, J.; Montelius, L.; Nicholls, I. A.; Omling, P.; Tagerud, S.; Mansson, A. *Biochem. Biophys. Res. Commun.* **2003**, *301*, 783–788.

(26) Sundberg, M.; Bunk, R.; Albet-Torres, N.; Kvennefors, A.; Persson, F.; Montelius, L.; Nicholls, I. A.; Ghatnekar-Nilsson, S.; Omling, P.; Tagerud, S.; Mansson, A. *Langmuir* **2006**, *22*, 7286–7295.

(27) Diez, S.; Reuther, C.; Dinu, C.; Seidel, R.; Mertig, M.; Pompe, W.; Howard, J. *Nano Lett.* **2003**, *3*, 1251–1254.

(28) Martinez-Neira, R.; Kekic, M.; Nicolau, D. V.; dos Remedios, C. G. *Biosens. Bioelectron.* **2005**, *20*, 1428–1432.

(29) Dennis, J. R.; Howard, J.; Vogel, V. *Nanotechnology* **1999**, *10*, 232–236.

(30) Brunner, C.; Ernst, K. H.; Hess, H.; Vogel, V. *Nanotechnology* **2004**, *15*, S540–S548.

(31) Manandhar, P.; Huang, L.; Grubich, J. R.; Hutchinson, J. W.; Chase, P. B.; Hong, S. H. *Langmuir* **2005**, *21*, 3213–3216.

(32) Sundberg, M.; Rosengren, J. P.; Bunk, R.; Lindahl, J.; Nicholls, I. A.; Tagerud, S.; Omling, P.; Montelius, L.; Mansson, A. *Anal. Biochem.* **2003**, *323*, 127–138.

(33) Suyama, K.; Miyamoto, Y.; Matsuoka, T.; Wada, S.; Tsunooka, M. *Polym. Adv. Technol.* **2000**, *11*, 589–596.

Table 1. Surface Properties and Motility Parameters on Respective Surfaces

surface	contact angle (deg)	surface tension (dyn/cm)	average height (nm)	area rms (nm)	average velocity ($\mu\text{m/s}$)	standard deviation of deflection angle
hydrophilic glass	36	56.3	1.83	0.109	no motility	
hydrophobic glass	48	48.1	0.61	0.096	2.29 (0.58)	17.64
PMMA	62	37.3	1.90	0.481	2.83 (0.72)	20.49
NC	67	39.0	1.93	0.588	3.33 (1.09)	14.57
AAPO	73	34.7	0.84	0.149	1.71 (0.48)	16.91
PtBuMA	78	329	3.24	0.679	No motility	—

a classical protocol.³⁴ A comprehensive description is provided in the Supporting Information.

First, HMM and actin were extracted from the back and leg muscles of a rabbit and purified by methods previously reported.³⁵ The actin filaments, obtained using a classical procedure,³⁶ were labeled with tetramethyl-rhodamine-phalloidin for fluorescence observation.

Second, flow cells for motility assays were built by sealing the test surfaces laterally with double-sided tape and a glass slide roof. For observation and recording, the flow cells were mounted on a fluorescence microscope (Nikon Eclipse TE300) with epifluorescence optics, a mercury light source, and a standard TRITC filter set (XF108-2, Omega Optical, Inc.; excitation: 500/550; emission: 560/650; dichroic: 555). The motility was observed at room temperature (23–25 °C). Images were recorded at 25 frames/s using an ISIS-3 intensified camera (Photonics Science, Ltd.). Particular attention was paid to rule out the possible impact of the diffusion of toxic small molecular species (e.g., residual monomers and solvents) from the polymer films. AAPO samples presented a slight motility-stalling effect, but the storage of samples for longer periods of time under vacuum and dry conditions resulted in normal motility.

Third, the coordinates of more than 20 actin filament heads in consecutive frames, obtained through manual tracking using Image-Pro (from Media Cybernetics) tracking capability, were statistically processed using Statistica Ver. 6.1 (StatSoft, Inc.) to calculate the motility statistics. To test the statistical validity of the results, and because a mismatch between the frame rate and the spatial resolution could lead to statistical artifacts,³⁷ we compared the motility statistics for nonaveraged data with those obtained by averaging the positions over two, three, and four frames and obtained similar statistical features for all cases, particularly the bimodality of the velocity distribution. As opposed to other studies,³⁸ we pooled the instantaneous velocities from all filaments, rather than calculating the average velocities per filament. Also, to rule out the impact of filament length on velocity,^{39,40} we processed only the trajectories of the filaments longer than 2 μm . These pooled statistical populations from the movement of different filaments have been further processed for statistical analysis. The *global* motility properties, that is, average velocity and smoothness of movement (standard deviation of velocity values), and *local* properties, that is, the acceleration and deflection angle (definitions presented in Supporting Information), were calculated. Finally, the trajectories of actin filaments have been color coded (red — start of the motion; purple — end of the motion) using a procedure described previously¹³ and an in-house developed software (Trajectoriser, freely available, see Supporting Information). The color coding avoids the possible confusion regarding the length of the trajectories (e.g., monocolored trajectories can be the result of long paths of short filaments or short paths of long filaments).

Protein Molecular Surfaces. The structures of 41 proteins were collected from the Protein Data Bank.⁴¹ The selected set of proteins

comprises several representative molecular motor proteins, including two structures of the S1 unit of myosin, one in the rigor state (2MYS) and one in the flexed state (1DFK), and an HMM structure (1B7T), as well as many other classes of unrelated proteins (i.e., lactalbumins, lysozymes, ribonucleases, hemoglobins, α -chymotrypsins, albumins, and antibodies).

Connolly's algorithm⁴² was used for the calculation of molecular surface properties for all selected proteins DS Viewer Pro software (from Accelrys, Inc.) was used for the visualization of several structures of the motor proteins. Briefly, the procedure for the quantification of molecular surface properties, which was described previously,⁴³ comprises the following steps: (i) if applicable, the structure of the probed protein is cleaned of water molecules, small chemical species, etc.; (ii) charges are assigned to atoms, according to the definitions used in classical force fields (Bio++ was used here, but other force fields produced similar results); (iii) a "virtual probing ball" with a radius chosen to match the probing object (e.g., water, solvent, adsorbing surface) is rolled over the molecular structure of the protein; (iv) the (x,y,z) coordinates of the points of contact between the protein structure and the probe are recorded; (v) partial charges are assigned to these coordinates, calculated as the ratio between the overall charge assigned to the respective atom and the area covered by the probe; (vi) calculations are made for the global molecular properties (i.e., total surface and total charges), surface densities (i.e., charge density calculated by dividing the total charge to the total molecular area), and specific surface properties (calculated by dividing the positive or negative charge to the positive and negative charged area, respectively). This procedure can be also used for the mapping of hydrophobicity, but all atoms belonging to an amino acid will be assigned the same hydrophobicity, resulting in less precise calculations. The use of probing balls with small radii, mimicking water or solvent molecules, will produce detailed molecular surface maps, while the use of probing balls with large radii, mimicking flat adsorbing surfaces, will result in patchy, noncontiguous molecular surfaces. The radius of the probe was chosen at 0.8 nm, which is within the range of average heights in Table 1. The use of larger radii did not significantly change the results of the quantification of molecular surface properties, but the calculations require far higher CPU times.

Further, the selected proteins were clustered using the calculated molecular surface properties as clustering dimensions and a cluster analysis algorithm (joining tree, single linkages, and Euclidian distances) as implemented in Statistica Ver. 6.1. software (from StatSoft Inc.). One set of proteins (hemoglobins) was chosen as a control set for the quality of the cluster analysis, because all the structures differed by a single amino acid.

3. Results and Discussion

Variation of Average Velocity with the Surface Hydrophobicity. The surfaces used to test the modulation of motility vary significantly in chemistry (Supporting Information Figure 1), have a moderate span of surface hydrophobicity (contact angle from 36° to 78°; Table 1), and have similarly flat

(34) Sellers, J. R.; Cuda, G.; Wang, F.; Homsher, E. In *Methods in Cell Biology*; Scholze, J. M., Ed.; Academic Press: San Diego, CA, 1993; Vol. 39, pp 23–49.

(35) Margossian, S. S.; Lowey, S. *Methods Enzymol.* **1982**, *85*, 55–71.

(36) Carsten, M. E.; Mommaerts, W. F. H. *Biochemistry* **1963**, *2*, 28–32.

(37) Uttenweiler, D.; Veigel, C.; Steubing, R.; Gotz, C.; Mann, S.; Haussecker, H.; Jahne, B.; Fink, R. H. A. *Biophys. J.* **2000**, *78*, 2709–2715.

(38) Toyoshima, Y. Y.; Kron, S. J.; McNally, E. M.; Niebling, K. R.; Toyoshima, C.; Spudich, J. A. *Nature* **1987**, *328*, 536–539.

(39) Toyoshima, Y. Y.; Kron, S. J.; Spudich, J. A. *Proc. Natl. Acad. Sci. U.S.A.* **1990**, *87*, 7130–7134.

(40) Sundberg, M.; Balaz, M.; Bunk, R.; Rosengren-Holmberg, J. P.; Montelius, L.; Nicholls, I. A.; Omeling, P.; Tägerud, S.; Månsson, A. *Langmuir* **2006**, *22*, 7302–7312.

(41) Berman, H. M.; Westbrook, J.; Feng, Z.; Gilliland, G.; Bhat, T. N.; Weissig, H.; Shindyalov, I. N.; Bourne, P. E. *Nucleic Acids Res.* **2000**, *28*.

(42) Connolly, M. L. *J. Mol. Graphics* **1993**, *11*, 139–143.

(43) Nicolau, D. V. J.; Fulga, F.; Nicolau, D. V. *Asia-Pacific Bioinformatics Conference (APBC2003)*; Chen, Y.-P., Ed.; Australian Computer Society: Darlinghurst, Australia, 2003; pp 29–34.

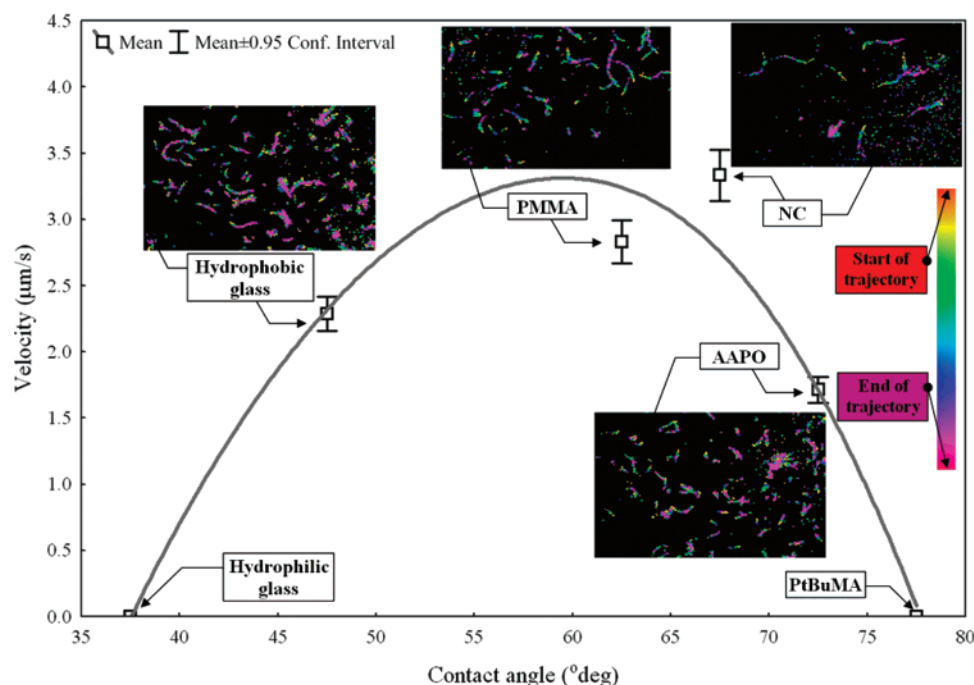


Figure 1. Average velocities of actin filaments (95% confidence error bars) on model surfaces that have different surface hydrophobicities. The insets represent the color-coded trajectories of the movement of actin filaments. The trajectories have been obtained by stacking sequential snapshots of actin filament position, each colored according its position in time (explanation of the colors in the color bar). Higher velocities (PMMA and NC) translate in longer trajectories; smoother translational movements (e.g., PMMA) result in clearer colored trajectories; and smoother directional movements (e.g., NC) result in straighter trajectories.

topographies (average heights spanning from 0.6 and 3.2 nm, compared with the approximate dimensions of the proteins immobilized on surfaces, i.e., HMM: tens of nanometers; BSA: 10–12 nm). Apparently, the surface hydrophobicity (i.e., contact angle) is the only factor that can be correlated with the motility characteristics (Figure 1). Within the limits of our experiments, the most hydrophilic and the most hydrophobic surfaces do not support the motility of actin filaments, but moderately hydrophobic surfaces provide a “motility window” (contact angles approximately between 50 and 73°) in which the average velocities vary from 1.5 to 3.5 $\mu\text{m/s}$ (maximum for NC surface).

It is important to note that minute and/or subtle differences in surface and protein preparation can lead to very different results for motility parameters. For instance, even for the standard surface NC, the reported average velocity spans from 7–8 $\mu\text{m/s}$ ^{38,44} to 4–5 $\mu\text{m/s}$.³⁹ Also, this work reports good motility on PMMA surfaces, in line with other contributions,^{9,16} while others^{10,25} used PMMA surfaces to deny motility confined actin filament movements. All the above variations can be accounted for by differences in HMM preparation, concentration of HMM in solution prior to immobilization, buffer conditions (in particular, ionic strength), and the method for the quantification of velocity. Particularly relevant for this study, different procedures for the preparation of surfaces, especially polymeric (e.g., casting solvent, bake cycle, storage), as well as different formulations of the same polymer (molecular weights and their distribution) can also lead to substantial differences in contact angle values. Consequently, it is conservatively justified to consider the surface-modulated variations of velocities within the same set of experiments, using identical experimental procedures and motor proteins.

Other Motility Parameters versus Surface Hydrophobicity.

The values of the standard deviation of velocity (Table 1), previously used to assess the smoothness of movement,⁴⁵ suggest that this is similarly modulated by surface hydrophobicity. However, a closer inspection of the color-coded trajectories in Figure 1 suggests more subtle differences in motility characteristics. While the length of the trajectory is proportional with the velocity, its thickness relates to the variations in the angle of movement. A more detailed description of the surface-induced modulation of motility parameters can be provided by the analysis of the distribution of instantaneous velocities, accelerations, and deflection angles. The acceleration is the first derivative of velocity, and the deflection angle measures the change in direction from one frame to another. Therefore, these two parameters (defined in the Supporting Information, Figure 2) quantify the translational and the angular smoothness of movement. At the limit, a perfectly uniform movement will present 0 values for the acceleration and deflection angle. The results of this analysis are presented in Figure 2 (and in Supporting Information, Figure 3). First, the velocity–acceleration bivariate histogram (left in Figure 2, and left column in Supporting Information, Figure 3) indicates that all velocity distributions comprise two clusters, for lower and higher velocities, respectively. For PMMA and NC, the velocities belong mostly to the high-velocity cluster, but the bimodal distribution of velocity is clearer on hydrophobic glass and AAPO. It appears that the average velocity (in Figure 1 and Table 1) is a result of the overlap and the relative weight of the average velocities in these two clusters. The distribution of instantaneous acceleration and deflection angle (Figure 2, right column, and middle and right columns in Supporting Information Figure 3) are also surface-specific. Most notably, PMMA presents the smoothest translational movement (narrow range of accelerations), and NC presents the smoothest directional movement

(44) Sundberg, M.; Balaz, M.; Bunk, R.; Rosengren-Holmberg, J. P.; Montelius, L.; Nicholls, I. A.; Omeling, P.; Tagerud, S.; Mansson, A. *Langmuir* **2006**, *22*, 7302–7312.

(45) Homsher, E.; Wang, F.; Sellers, J. R. *Am. J. Physiol.* **1992**, *262*, C714–C723.

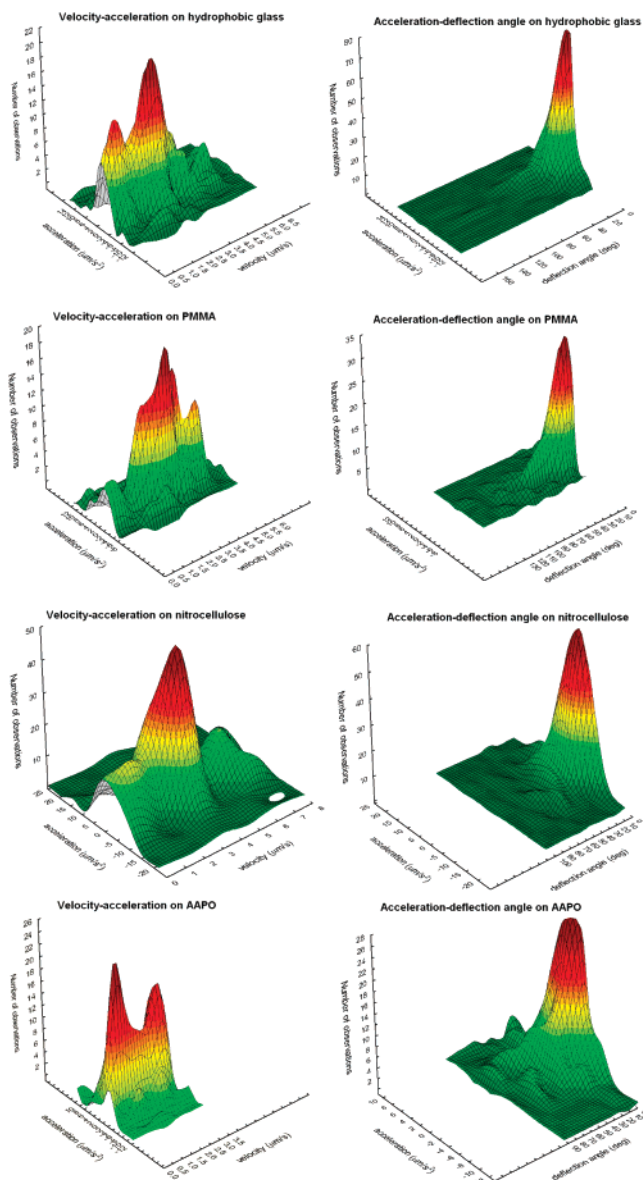


Figure 2. Bivariate histograms of the motility parameters of actin filaments on model surfaces: velocity vs acceleration (left column) and deflection angle vs acceleration (right column). The bimodality of velocity is more apparent for motility on hydrophobic glass and AAPO.

(narrow range of deflection angles). Several studies^{45,46} reported similar bimodality of velocity, but this is difficult to reveal if the instantaneous velocities are averaged per filament³⁸ rather than pooled together as in the present study.

Considerations Regarding Molecular Surfaces. Because of the high sensitivity of motor proteins, the motility assays and related nanodevices have to be operated in highly optimized fluid conditions and on surfaces that are optimal for motility. In general, the adsorption and behavior of proteins immobilized on surfaces is modulated by (i) protein properties (e.g., hydrophobicity, charges, and their distributions on the molecular surface, as well as molecular weight and protein flexibility), (ii) properties of the adsorbing surface (i.e., surface tension, chemistry, and possibly nanotopography), and (iii) the properties of the fluid environment (i.e., pH, ionic strength, and temperature). Of these three sets of process parameters, the first is the most complex

to quantify, hence a study of the molecular surface of the motor proteins, as probed by an adsorbing surface, is fully warranted. Figure 3 presents both a qualitative and quantitative analysis of the differences between the two extreme states of myosin (S1 unit) in the form of visualization of molecular surfaces and cluster analysis.

First, the comparison of the molecular surfaces of two extreme conformations of the S1 unit as probed by an adsorbing surface; that is, a large probing ball radius (top left corner in Figure 3) leads to the qualitative realization that these structures are extremely different. For instance, one limit structure (1DFK) has a larger contact area, whereas the other (2MYS) has a more uneven distribution of properties on the molecular surface. Therefore, the S1 unit (and, by extension, myosin) is in a sense a “bimodal” protein, quickly switching between two very different conformations. If the two conformations of the S1 unit are standalone proteins, it would be expected that 1DFK will adsorb more on surfaces (larger/more hydrophobic areas), and 2MYS will denature more (as a result of preferential adsorption of selected sites leading to local conformational changes).

Second, a quantitative analysis is offered by the clustering of 41 proteins, according to their total charges and their density and distribution (Figure 3, right-hand corner). The nature of the proteins is not an input to the clustering algorithm, which uses only the molecular surface properties as clustering dimensions. Therefore, the accuracy of the clustering methodology is demonstrated by the correct clustering of the classes of proteins, particularly hemoglobins (the control cluster, in the middle of the clustering triangle). The central assumption that motivated the cluster analysis is that similar proteins, in identical conditions (same adsorbing surface and fluid medium), will adsorb similarly and will have similar surface-modulated bioactivity. Revealingly, the analysis shows that the flexed S1 structure (1DFK) has the highest dissimilarity in the protein population, even compared to the S1-rigor conformation and HMM with both heads in rigor state (1B7T).

The logical conclusion following this extreme dissimilarity between the S1 structures means that it is very difficult to find a surface that is optimal for *both* rigor- and flexed-state conformations. Consequently, and regardless of the nature of the surface, it is likely that HMM molecules with the heads close to, or touching the surface will partially or totally lose their bioactivity if one or both arms are affected, respectively.

Considerations Regarding Protein Adsorption and Denaturation. Protein adsorption on solid surfaces is a phenomenon that is important to a number of biomedical applications, ranging from biomaterials to protein arrays and lab-on-a-chip devices. Unfortunately, despite this general and acute interest, periodically reviewed in comprehensive works,^{47–49} protein adsorption remains a very complex process that has, for the most part, resisted efforts to predict it from the first principles with a reasonable degree of accuracy. Several decades of research resulted, however, in the acceptance of some general rules regarding protein adsorption, applied here to motor proteins immobilized on surfaces. First, hydrophobic surfaces amplify the amount of adsorbed proteins, but also increase their level of conformational change,^{50,51} even for robust ones such as lysozyme.^{52,53} Particularly relevant in the context of protein molecular motors

(47) Horbett, T. A.; Brash, J. L. *Proteins at Interfaces II: Fundamentals and Applications*; American Chemical Society: Washington, DC, 1995; Vol. 602.

(48) Hlady, V.; Buijs, J. *Curr. Opin. Biotechnol.* **1996**, 7, 72–77.

(49) Nakanishi, K.; Sakiyama, T.; Imamura, K. *J. Biosci. Bioeng.* **2001**, 91, 233–244.

(50) Haynes, C. A.; Norde, W. *J. Colloid Interface Sci.* **1995**, 169, 313–328.

(51) Ostuni, E.; Grzybowski, B. A.; Mrksich, M.; Roberts, C. S.; Whitesides, G. M. *Langmuir* **2003**, 19, 1861–1872.

(46) Marston, S. B.; Fraser, I. D. C.; Bing, N.; Roper, G. J. *Muscle Res. Cell Motil.* **1996**, 17, 497–506.

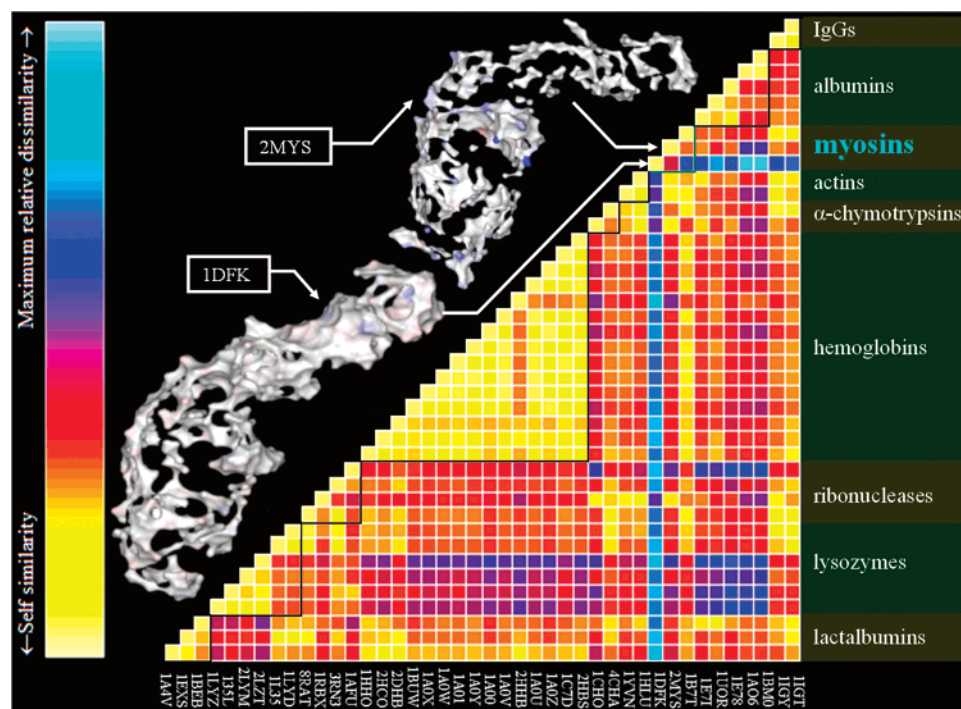


Figure 3. Clustering of 41 different proteins, including two structures of the S1 unit (1DFK and 2MYS) and HMM (1B7T), using molecular surface properties calculated with atomic-level resolution as clustering dimensions. The bar on the right represents the level of relative similarity (yellow: self-identical structures; turquoise: most dissimilar structures). The molecular surfaces of S1 units (probing ball radius of 0.8 nm), in flexed state (1DFK, bottom left) and rigor state (2MYS, top left) are also presented (blue areas: positively charged domains). The position of these proteins in the comparative distance matrix is indicated by arrows.

adsorbed on surfaces is that the driving force for adsorption is the dehydration of both the hydrophobic adsorbing surface and the protein molecular surface.⁵¹ Because the function of molecular motors is critically linked to the structuring of water around the point of contact between the motor and the filament,⁵⁴ the hydrophobic-surface-induced dehydration of the protein may represent an additional, different type of denaturation (i.e., loss of function), rather than natural conformation. Second, hydrophilic surfaces repel proteins, although this has to be qualified; a comprehensive study⁵⁵ using self-assembled monolayers to probe protein adsorption found that the surfaces that resist the adsorption of proteins incorporate groups that exhibit four molecular-level characteristics: (i) they are hydrophilic, (ii) they include hydrogen-bond acceptors, (iii) they do not include hydrogen-bond donors, and (iv) their overall electrical charge is neutral. Hydrophilicity aside, with the exception of hydrophilic glass, the last three rules apply to all surfaces (Supporting Information, Figure 1). Hydrophilic surfaces can also induce the denaturation of the adsorbed proteins,⁵⁰ provided that they are considerably charged, but this does not seem to be the case for the surfaces used in this study. It is reasonable to assume that, in the context of this study, the level of adsorption and denaturation on hydrophilic surfaces is less than that on hydrophobic ones. Third, all things being equal, a pH of the buffer close to the isoelectric point of the protein will have an effect similar to that of hydrophobic surfaces, that is, it will induce the highest amount of adsorbed protein because of the decrease of the charging on the protein molecular surface and the subsequent decrease of

hydrophobicity. Conversely, a high ionic strength of the buffer will have the opposite effect, by shielding the protein molecular surface and rendering it more hydrophilic. This latter aspect, which can be the source of important differences between reported data on motility assays, has been explored before⁴⁵ and recently.^{44,56}

Compared with other bioassays with surface-immobilized proteins, the motility assays pose specific additional problems. In classical protein assays (e.g., antibody assays), the proteins on the surface are either active or denatured, that is, preserving or not preserving their biomolecular recognition capabilities, respectively. In actin–myosin motility assays, however, the protein motor molecules can be classified in populations having different levels of bioactivity and in ever-decreasing numbers of molecules: total number of motors > number of motors that are ATP-active > number of motors that are capable of ensuring the motility of filaments (i.e., operating with either one or both heads) = (number of motors operating with full motility capacity, i.e., operating with both heads) + (those operating with a single head). While the number of ATP-active molecules can be measured by classical ATPase assays,^{39,57} and there were recent attempts to also measure the total number of proteins,^{44,56,58} the number of motility-able motor molecules could not be determined unequivocally, let alone the ratio between the motors working with one or two heads. However, because, during their movement, the heads of actin filaments visit individual sites where motors with different working modes are localized, the statistical analysis of the instantaneous motility parameters presented above can be

(52) Lu, J. R.; Su, T. J.; Thirtle, P. N.; Thomas, R. K.; Rennie, A. R.; Cubitt, R. *J. Colloid Interface Sci.* **206**, 212–223.

(53) Wertz, C. F.; Santore, M. M. *Langmuir* **2002**, *18*, 1190–1199.

(54) Kabir, S. R.; Yokoyama, K.; Mihashi, K.; Kodama, T.; Suzuki, M. *Biophys. J.* **2003**, *85*, 3154–3161.

(55) Ostuni, E.; Chapman, R. G.; Holmlin, R. E.; Takayama, S.; Whitesides, G. M. *Langmuir* **2001**, *17*, 5605–5620.

(56) Balaz, M.; Sundberg, M.; Persson, M.; Kvassman, J.; Mansson, A. *Biochemistry* **2007**, *46*, 7233–7251.

(57) Harris, D. E.; Work, S. S.; Wright, R. K.; Alpert, N. R.; Warshaw, D. M. *J. Muscle Res. Cell Motil.* **1994**, *15*, 11–19.

(58) Hanson, K. L.; Viidyanathan, V.; Nicolau, D. V. *BioMEMS and Nanotechnology II*; Nicolau, D., Ed.; SPIE Publications: Bellingham, WA, 2006; pp 12–19.

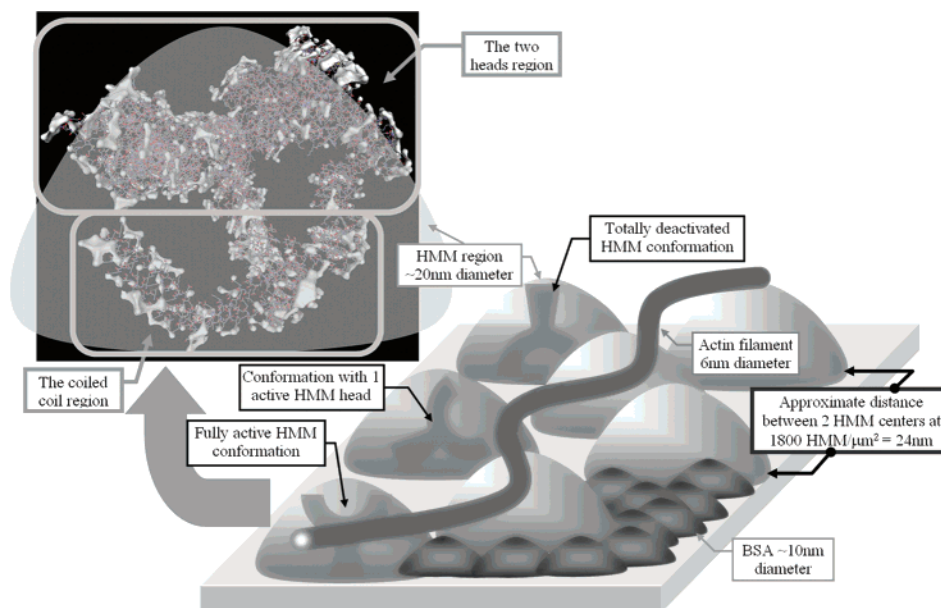


Figure 4. Proposed schematic model of the distribution and possible orientations of HMM on surfaces. The volumes occupied by HMM, blocking proteins (e.g., albumin), and actin filaments are presented with their approximate relative dimensions. The maximum surface defect heights (not figured) are 2 nm (Table 1), which is approximately 5 times smaller than BSA dimensions. The inset presents the HMM molecular structure. The gray patches represent the areas of contact between the protein surface and a probe with a large (2 nm) radius, which mimics the adsorption surface. For comparison purposes, the approximate semispherical volume of the HMM in the scheme on the right is also overlapped with the molecular structure.

used as a basis for a model regarding the individual operation of an actin–myosin tandem.

Motility Processes Modulated by Surface Properties. The above results and discussion allow the formulation of a tentative model describing the surface-modulated, myosin II-propelled motility of actin filaments.

(i) While the filament's movement velocity is a result of the number of heads operating along the filament, the ratio between active and inactive heads, and filament length,⁵⁹ the movement itself is controlled by the head of the filament which has to come in contact with an active HMM head. If the head of the actin filament cannot find an active head, it "searches" the surrounding area by Brownian motion until one is found and the movement is unlocked. Therefore, the head of the actin filament is spatially probing the existence and the state of the HMM head(s), and, consequently, the statistical analysis of instantaneous motility parameters can provide information about HMM populations.

(ii) The motility of actin filaments is modulated by surface hydrophobicity: a higher total surface density of HMM heads should occur on more hydrophobic surfaces, and a higher ratio of active, nondenatured HMM heads should occur on more hydrophilic surfaces. Some denatured heads will still be able to attach to the filament, but they might be unable to propel it, resulting in an apparent drag force applied on the filament.

(iii) The random character of protein adsorption will result in three generic conformations of surface-adsorbed HMM (as proposed in Figure 4). Consequently, there are three HMM populations, that is, HMM with (i) both heads active (generating a high velocity per filament unit, within 3–8 $\mu\text{m/s}$), (ii) one head active (low velocity per unit head; it has been demonstrated^{38,60} that the S1 unit of myosin II can propel the actin filament with only one head, albeit with lower velocities (around 1–2 $\mu\text{m/s}$)),

and (iii) HMM unable to propel actin filaments because of surface-induced denaturation.

The proposed model allows the interpretation of experimental observations. First, on hydrophilic surfaces outside the "motility window" (hydrophilic glass), the total concentration of the population of active motors is below a critical level needed for motility because of the large distances between isolated heads. At the other extreme, the too hydrophobic surface (PtBuMA) denatures too many HMM molecules with the same result: large distances between motile-able heads. Second, the surfaces at the "motility window" boundaries (AAPO and hydrophobic glass) will have a concentration of active HMM heads above the required critical level, but will also present a significant proportion of HMM molecules working with one head. Third, the surfaces in the middle of the "motility window" (PMMA and NC) will present a higher proportion of HMM molecules working with two heads. This model complements previous observations,^{57,61–63} including those reporting the bimodality of velocity,^{45,46} and gives a molecular interpretation for the existence of the bimodal behavior of actomyosin motility.

The present model also complements the Julicher and Prost model,⁶⁴ which is based on very different considerations, and which proposes that oscillatory motion of molecular motors cooperating in large groups occurs when the system is elastically coupled to its environment. This stochastic model suggests that minute differences in the collective behavior of the motor population, especially at high concentrations, can result in a change in directionality. This model has been used to explain the existence of two populations of actin filaments, moving in opposite directions in very confined spaces, despite the strong electrophoretic pull applied on them if they move in one direction

(61) Tawada, K.; Sekimoto, K. *Biophys. J.* **1991**, *59*, 343–356.

(62) Cuda, G.; Pate, E.; Cooke, R.; Sellers, J. R. *Biophys. J.* **1997**, *72*, 1767–1779.

(63) Bourdieu, L.; Magnasco, M. O.; Winkelmann, D. A.; Libchaber, A. *Phys. Rev. E* **1995**, *52*, 6573–6579.

(64) Julicher, F.; Prost, J. *Phys. Rev. Lett.* **1997**, *78*, 4510–4513.

(59) Uyeda, T. Q. P.; Kron, S. J.; Spudich, J. A. *J. Mol. Biol.* **1990**, *214*, 699–710.

(60) Shaffer, J. F.; Razumova, M. V.; Tu, A.-Y.; Regnier, M.; Harris, S. P. *FEBS Lett.* **2007**, *581*, 1501–1504.

only.¹⁰ It is reasonable to expect that the existence of several populations of propellers will also exacerbate the instability of the actomyosin system and will result in a bimodal motility behavior.

It is interesting to corroborate our results and proposed model with other reported data. While only few studies have briefly touched the subject of surface-induced modulation of the motility of actin filaments,^{13,32} recent comprehensive studies^{32,44} have compared the motility behavior modulated by the hydrophobicity of semiconductor-derived hard surfaces. It has been shown that the velocity increases with surface hydrophobicity, up to contact angles of 80° (i.e., above the ranges of surface hydrophobicities presented in this work), rather than decreasing for high surface hydrophobicities. Apart from several qualifications regarding the differences in protein purification and the measurement of surface hydrophobicity mentioned in a previous section, this difference in observed trends deserves further, more detailed analysis, as follows: First, these two studies used markedly different types of hydrophobic surfaces, that is, semiconductor-derived surfaces⁴⁴ and polymers (in the present work), which are molecularly hard and molecularly soft surfaces, respectively. The study of the adsorption and behavior of proteins on polymers has always been challenging, because it is essentially impossible to define a clear boundary between the protein and polymer domains (a non-issue for molecularly hard surfaces). Also, the dynamic features of the system, the structure of the polymer surface before and after adsorption, the area of the surface that was involved, and the structure (or range of structures) of the protein after adsorption, are essentially intractable.⁵¹ It is clear, however, that the hydrophobic effects constitute the most important interaction between the surface and the protein. Second, studies on the interfacial rheological properties of adsorbed protein layers on molecularly flexible interfaces⁶⁵ demonstrated that myosin is the protein with the greatest internal cohesion and structuring of all tested proteins, some of which are used as blocking agents in motility assays (e.g., albumin, casein). As this information refers to the whole myosin, which contains a large, noncompact coiled coil domain, we can infer that the heads have a very high internal cohesion. Therefore, it can be argued that, on molecularly flexible surfaces, the blocking proteins are less successful in shielding the contact between HMM heads and the polymeric chains. Conversely, on molecularly hard surfaces, the blocking function of neutral proteins is more effective, and, consequently, the motors will be more resistant to surface-induced denaturation. For even larger surface hydrophobicities (contact angles higher than 80–90°), one would expect a similar trend (a decrease in average velocities).

Significance of the Design, Fabrication, and Operation of Dynamic Nanodevices. Future dynamic nanodevices based on protein molecular motors are expected to find applications as diagnostic devices and biosensors, but also in information processing and storage, nanotransport, and construction. These devices will essentially be very large parallel systems of individual single-molecule devices working independently or coordinated. A lot of progress has been made in the past decade regarding the global engineering of the molecular motor-based devices, e.g., molecular selectors and rectifiers, electrophoretic steering, and so forth, but less attention has been paid to how motile objects behave individually.

Different devices would require different characteristics of the molecular motors. For instance, the need for rapid transduction would warrant the actomyosin system, which can deliver high velocities, whereas the need for precisely modulated bidirectional

movement would warrant the microtubule-based motors. Whatever the global technical solution, as required by the specific application, one common, critical condition is that individual motile nano-objects (beads, simple or decorated actin filaments, or microtubules) operate identically or, at the very least, predictably; the lack of randomness and variability are preconditions for the design, fabrication, and operation of engineered devices and systems. It follows that the smoothness of movement is required for all molecular motor-based devices, and, for devices performing repetitive directional tasks,^{20,66} the smoothness of movement is also critical. The challenge is therefore to find those conditions that will ensure the optimal operation (e.g., velocity), but equally quasi-identical operation of these independent devices. Another, separate challenge is the selection of materials amenable for device fabrication and operation.

The present study suggests that PMMA is a very good candidate for the actomyosin-based nanodevices because (i) it allows good motility characteristics of the actin filaments, that is, sufficiently high average velocities, and smooth translational movement, and (ii) it is an excellent fabrication material for both nanolithography (e.g., classical e-beam and novel ion-beam nanolithography⁶⁷) and, more recently, nanoimprint lithography⁶⁸ and microfluidic devices (e.g., easy functionalization⁶⁹ and low fluorescence background and high transparency⁷⁰). The larger variability of the deflection angles can be managed, where required, through micro or nanofabricated structures, as it has been demonstrated before for PMMA.^{9,13,16} In addition, this study demonstrates that PMMA is also an excellent material from the operational perspective, because it presents a quasi-monomodal distribution of the propellers. Finally, given the relative large dimensions of HMM and easy functionalization procedures of PMMA surfaces,⁶⁹ it would be possible to perform some *vertical* nanoengineering (as opposed to the already well-developed horizontal using appropriately shaped rectifiers,^{15,16,26} for instance, mounting individual HMM heads on elevated nanostructures via functionalization with myosin antibodies,^{10,63,71} which in turn will allow the full detachment of motility behavior from surface effects.

4. Conclusion

This contribution demonstrates the need (and the possibility) of the optimization of surfaces for future dynamic nanodevices based on protein molecular motors. It has been found that small variations in hydrophobicity, especially for polymer surfaces, translate into large variations of motility characteristics. The analysis of motility and molecular surfaces has been used to assess the appropriateness of several mildly hydrophobic polymers, of which PMMA is a very good candidate for actomyosin-based nanodevices. The study also proposes an engineering-oriented assessment methodology focused on individual, rather than global, behavior of motile elements and stresses the need for the minimization of the variability for future dynamic nanodevices.

(66) Hess, H.; Matzke, C. M.; Doot, R. K.; Clemmens, J.; Bachand, G. D.; Bunker, B. C.; Vogel, V. *Nano Lett.* **2003**, *3*, 1651–1655.

(67) Bruenger, W. H.; Buschbeck, H.; Cekan, E.; Eder, S.; Fedynyshyn, T. H.; Hertlein, W. G.; Hudek, P.; Kostic, I.; Loeschner, H.; Rangelow, I. W.; Torkler, M. *Microelectron. Eng.* **1998**, *42*, 237–240.

(68) Taniguchi, J.; Tokano, Y.; Miyamoto, I.; Komuro, M.; Hiroshima, H. *Nanotechnology* **2002**, *13*, 592–596.

(69) Fixe, F.; Dufva, M.; Telleman, P.; Christensen, C. B. V. *Lab Chip* **2004**, *4*, 191–195.

(70) Piruska, A.; Nikcevic, I.; Lee, S. H.; Ahn, C.; Heineman, W. R.; Limbach, P. A.; Seliskar, C. J. *Lab Chip* **2005**, *5*, 1348–1354.

(71) Winkelman, D. A.; Bourdieu, L.; Ott, A.; Kinose, F.; Libchaber, A. *Biophys. J.* **1995**, *68*, 2444–2453.

(65) Bos, A. M.; van Vliet, T. *Adv. Colloid Interface Sci.* **2001**, *91*, 437–471.

Acknowledgment. The research has been supported by grants from Defense Advanced Research Projects Agency (DARPA), Australian Research Council and FP6 Integrated Projects. We thank Drs. K. Suyama, M. Shirai and M. Tsunooka from Osaka Prefecture University for AAPO polymer.

Supporting Information Available: Chemical structures of the materials used, additional statistical data regarding motility, examples of motility assays movies, and detailed motility protocol. This material is available free of charge via the Internet at <http://pubs.acs.org>.

LA700412M